SUPPLEMENTAL INFORMATION

RnhP is a plasmid-borne RNase HI that contributes to genome maintenance in the ancestral strain *Bacillus subtilis* NCIB 3610

Taylor M. Nye[1], Emma K. McLean[1], Andrew M. Burrage[2], Devon D. Dennison[1], Daniel B. Kearns[2], and Lyle A. Simmons[1,*]

[1]Department of Molecular, Cellular, and Developmental Biology
University of Michigan, Ann Arbor, Michigan USA.
[2]Department of Biology, Indiana University, Bloomington, Indiana, USA

To whom correspondence should be addressed: Department of Molecular, Cellular, and Developmental Biology, University of Michigan, Ann Arbor, Michigan 48109-1055, United States. Phone: (734) 647-2016, Fax: (734) 615-6337
E-mail: lasimm@umich.edu

Running Title: RnhP is a plasmid-borne RNase HI
Keywords: RNase HI, SOS, RNA-DNA hybrid, *Bacillus subtilis*, NCIB 3610

SUPPLEMENTAL EXPERIMENTAL PROCEDURES

Strain construction: Chromosome deletion strains were created by transforming competent DK1042 cells (Nye *et al.*, 2017) with genomic DNA purified from *Bacillus subtilis* 168 strains with the gene of interest replaced by an erythromycin resistance cassette flanked by *loxP* sites obtained from the Bacillus Genetic Stock Center (http://www.bgsc.org/). The erythromycin resistance cassette was subsequently removed with Cre recombinase (Koo *et al.*, 2017).

To generate the Δ*rnhP* in-frame markerless deletion plasmid pAMB32 was constructed. The region 5' to *rnhP* was amplified using the primer pair 6715/6716 and subsequently digested with HindIII and SalI, and the region 3' of *rnhP* was amplified with primer pair 6717/6718 and digested with SalI and KpnI. The two fragments were simultaneously ligated into HindIII/KpnI-digested pMiniMAD2, which contains a temperature-sensitive origin of replication and an erythromycin resistance cassette (Patrick & Kearns, 2008). *Escherichia coli* TG1 was transformed with the resulting product to generate pAMB32. The pAMB32 plasmid was introduced into DK1042 by transformation at the permissive temperature for plasmid replication (22°C) using mls resistance as a selection. The resulting strain (DK7021) was grown on plates containing mls at the restrictive temperature for plasmid replication (37°C) to force integration of the extra-chromosomal plasmid into pBS32. To evict the plasmid, the strain was incubated in 3 mL LB at the permissive temperature for 14h, diluted 30-fold in fresh LB, and incubation continued at the permissive temperature for another 24h. Cells were serially diluted and plated on LB agar at 37°C. Individual colonies were replica patched onto LB plates ad LB plates containing mls to identify mls-sensitive colonies that evicted the plasmid. Colonies that

had evicted the plasmid were screened by PCR using primers 6715/6718 to assess which isolates retained the Δ*rnhP* allele.

The *tagC::tagC-gfp* reporter strains were created by transforming genomic DNA purified from *tagC::tagC-gfp* in *B. subtilis* PY79 (KJW7) into the appropriate background and verified via resistance to the selectable marker spectinomycin and microscopy (Britton & Grossman, 1999). The inducible *sigN* strains were created by transduction with lysate from DK1634 and subsequently verified (Yasbin & Young, 1974).

The *ppsA-E* deletion was created using the CRISPR-Cas method developed previously (Burby & Simmons, 2016, Burby & Simmons, 2017). Briefly, primers oTMN75 and oTMN76 were used to generate the protospacer motif designed to target Cas9 within the *ppsB* gene. The protospacer motif was then ligated into pPB105 as described (Burby & Simmons, 2016, Burby & Simmons, 2017). The editing template was created by amplifying the regions 1 kb upstream of *ppsA* and downstream of *ppsE* with primer sets oTMN77/oTMN78 and oTMN79/oTMN80, respectively. Fragments for the plasmid, the *ppsA* upstream, and the *ppsE* downstream region were ligated together via Gibson assembly to create plasmid pTNDpps. pTNDpps was transformed into competent *B. subtilis* strains and transformants were selected via resistance to chloramphenicol. Following colony purification, the strains were cured of the plasmid via growth at 42°C.

DNA sequencing and chromosome coverage analysis for *ppsA-E* deletion experiments: Library preparation and DNA paired-end sequencing was performed by the University of Michigan DNA Sequencing Core. Sequencing reads were aligned using bowtie2 (v 2.3.5.1) to the NCIB 3610 chromosome reference (CP020102.1) (Li & Durbin, 2009, Nye *et al.*, 2017). The resulting sam files were converted to bam files, sorted, and

filtered using samtools (v 1.10) for quality values greater than 30 (Li *et al.*, 2009). PCR duplicates were removed using Picard tools (v 2.23.0) (https://github.com/broadinstitute/picard). The filtered bam files were used to calculate the genome coverage at each base for each replicate using genomeCoverageBed from bedtools (v 2.29.1) (Quinlan & Hall, 2010). The coverage at each base was averaged for the three replicates. The median coverage over 10kb windows was plotted every 1kb throughout the length of the chromosome using the packages ggplot2 and zoo in R (v 3.1.3) (Wickham, 2016, Zeileis & Grothendieck, 2005).

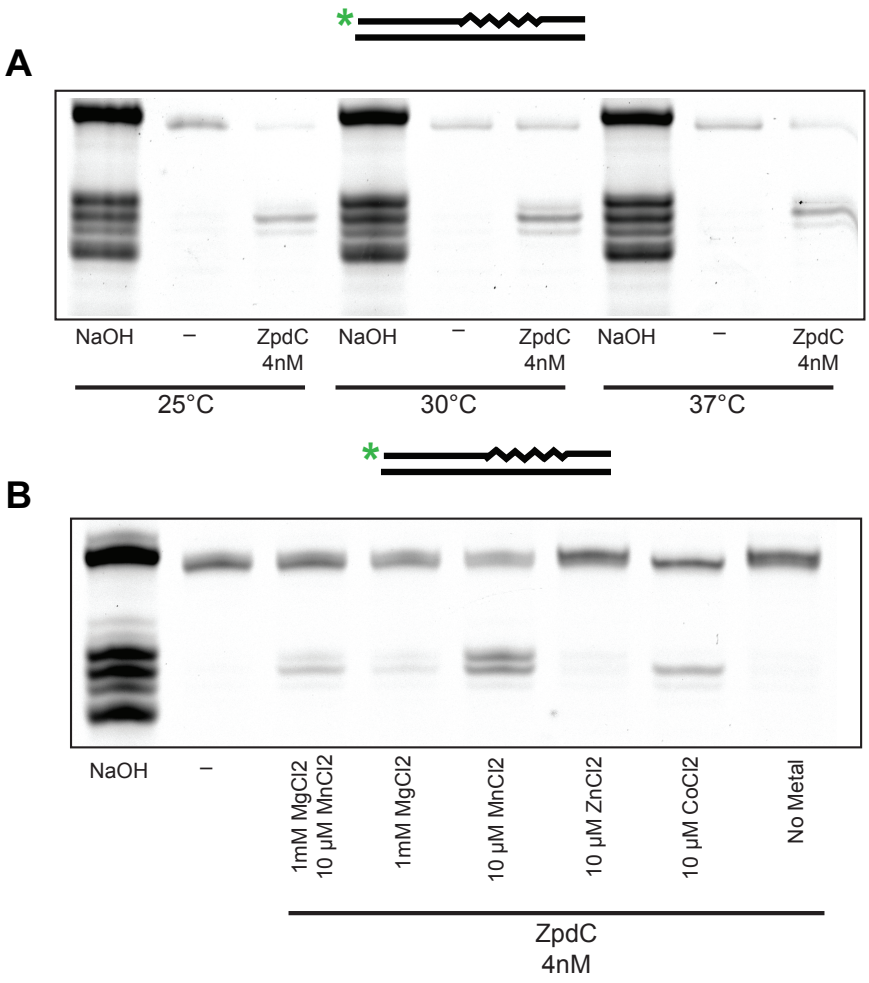

Figure S1. ZpdC (RnhP) is active at various temperatures and prefers Mn^{2+} as a metal cofactor. (A) RnhP was incubated in reaction buffer (see Experimental Procedures) with the ribopatch substrate at the indicated temperatures for ten minutes. A 5' end IR-labeled oligo containing 4 embedded rNMPs (squiggly lines) within an otherwise DNA oligo (straight lines) was annealed to a complementary DNA oligo (oJR210 and oJR145) and treated with 4 nM RnhP at the indicated temperatures. **(B)** RnhP was incubated with the ribopatch substrate described in (A) in a reaction buffer (20 mM Tris-HCl pH8, 50 nM NaCl, and 1 mM DTT) containing the indicated concentrations of metal ions. For both experiments, a ladder was created via alkaline hydrolysis of the substrate at the embedded rNMPs (lane one). The products were separated on a 20% denaturing urea-PAGE gel and subsequently visualized with a LI-COR Odyssey imager.

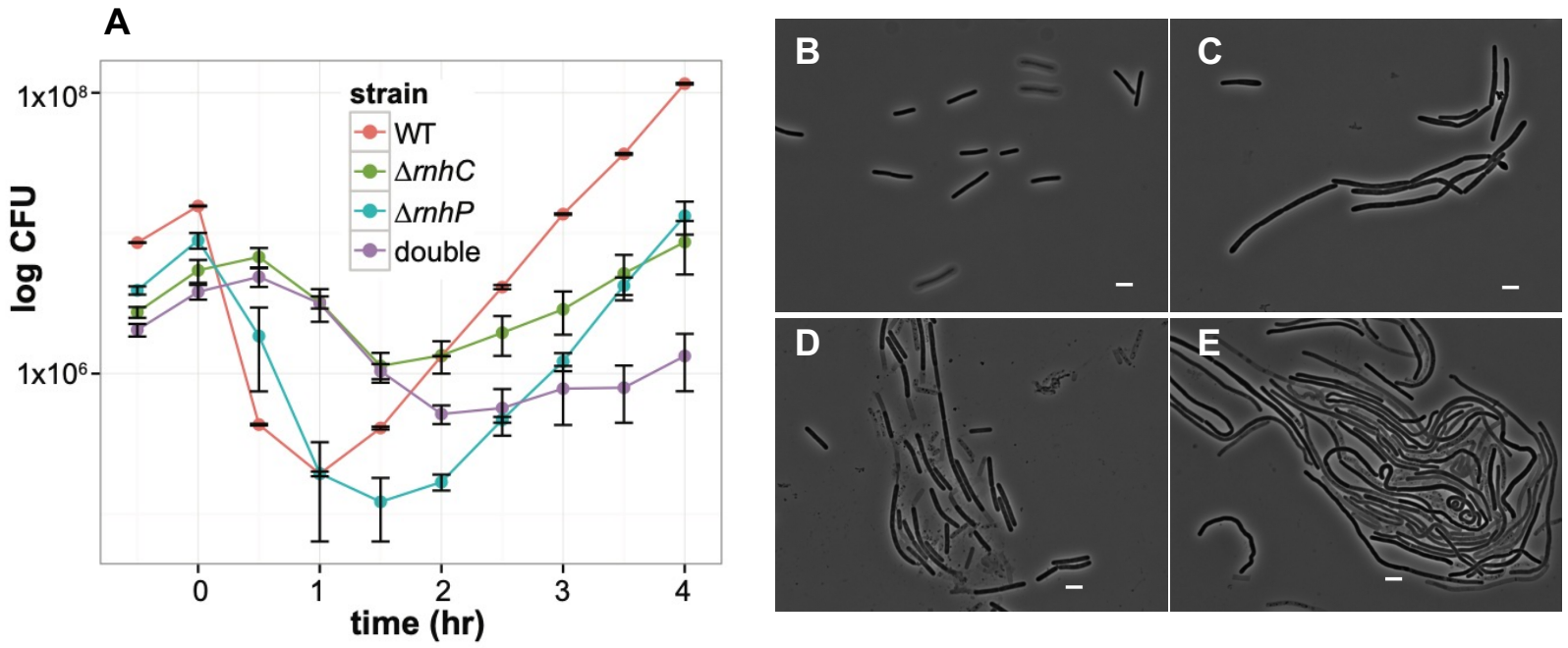

Figure S2. Plasmid mediated cell death and cell elongation are affected by induction of plasmid hyper-replication in the absence of RnhC but not RnhP. (A) Average colony forming units (y-axis) for three replicates of *sigN* inducible strains in WT, Δ*rnhC*, Δ*rnhP*, and Δ*rnhP rnhC::erm* backgrounds over time (x-axis). The standard errors are indicated. **(B-C)** Representative images for IPTG inducible *sigN* strains in WT and Δ*rnhP rnhC::erm* backgrounds pre-induction with IPTG, respectively. **(D-E)** Representative images for IPTG inducible *sigN* strains in WT and Δ*rnhP rnhC::erm* backgrounds 4 hours post induction with IPTG, respectively.

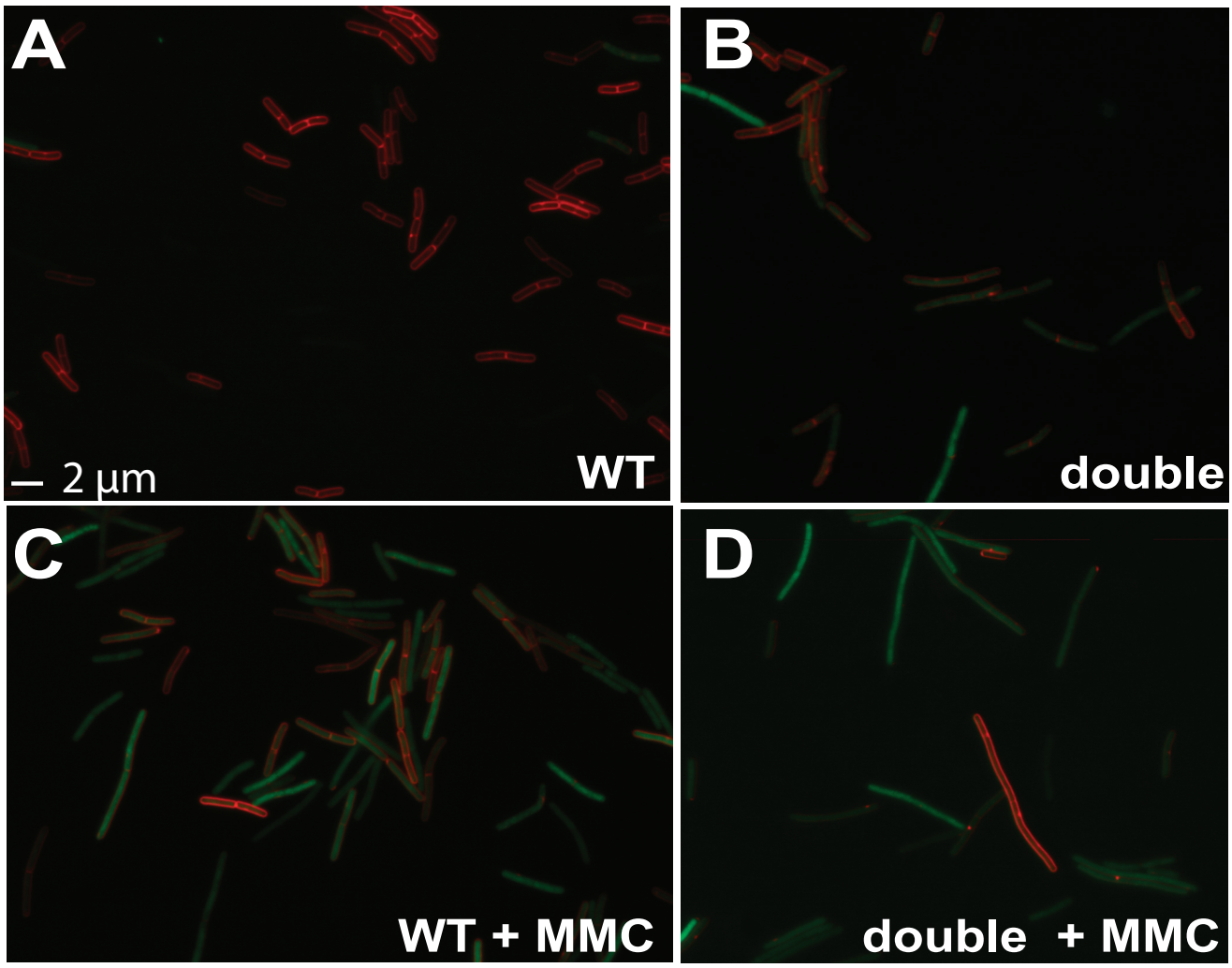

Figure S3. Loss of RnhP and RnhC activates the SOS response under normal growth conditions. (A-B) Representative images for *tagC::tagC-gfp* reporter strains in WT and Δ*rnhP rnhC::erm* backgrounds. **(C-D)** Representative images for *tagC::tagC-gfp* reporter strains in WT (3610) and Δ*rnhP rnhC::erm* backgrounds plus treatment with mitomycin C.

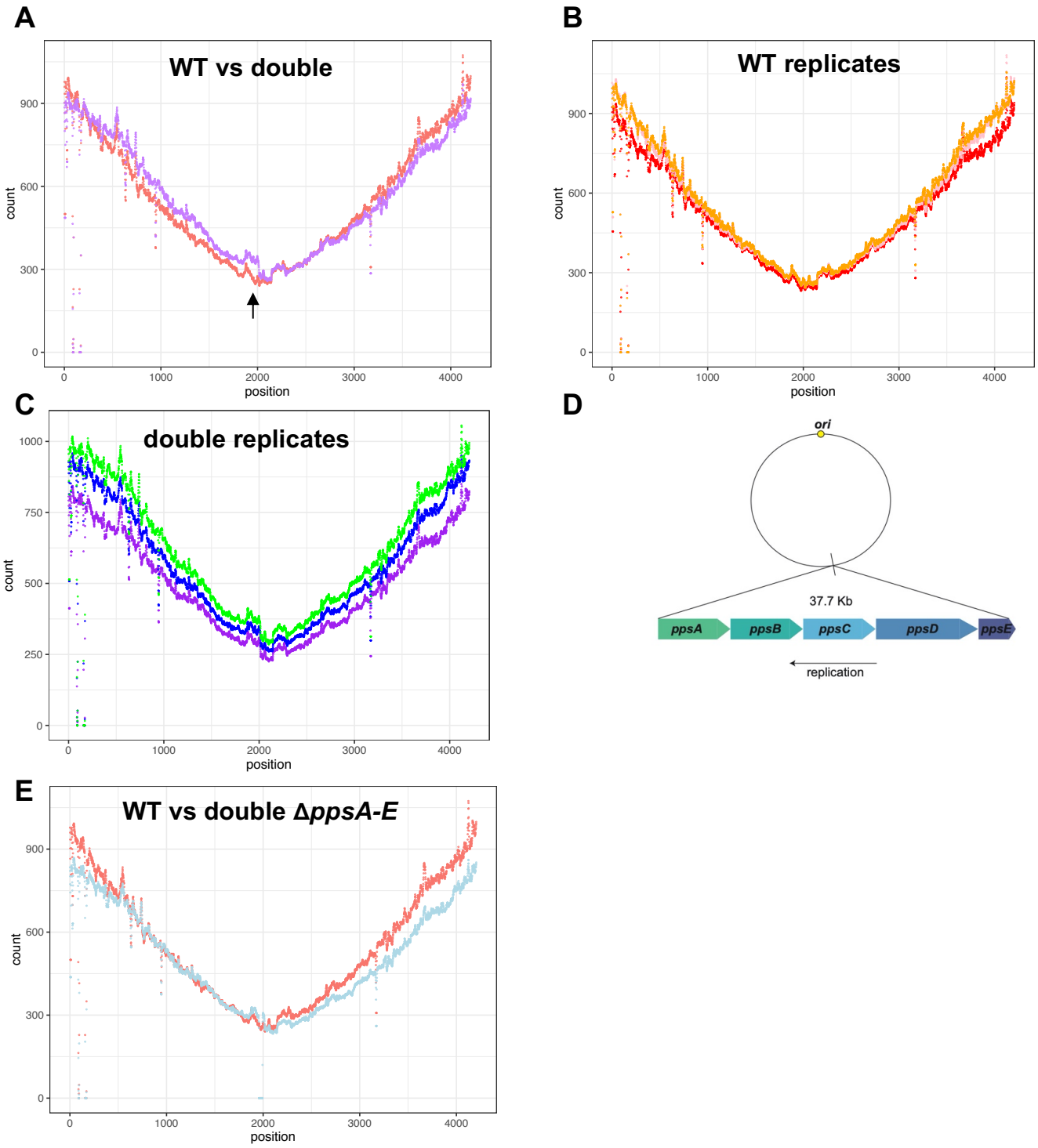

Figure S4. Deletion of *ppsA-E* mitigates laggard replication progression around the terminus in cells lacking *rnhP* and *rnhC* genes. Average genome coverage of exponentially growing cells. Average count of sequencing coverage at each base (y-axis) for three independent replicates with reads aligned to the NCIB 3610 reference genome (Nye *et al.*, 2017) chromosome over 10 Kb regions is plotted in 1Kb sliding windows over the length of the chromosome (x-axis). The first origin proximal base in the reference genome represents position 1. The median value across each

window was plotted. **(A)** Average genome coverage of WT (pink) and Δ*rnhP rnhC::erm* (purple) strains. The *ppsA-E* locus (1,960,230 – 1,997,989) is indicated by a black arrow. **(B)** Genome coverage of three biological replicates for WT. **(C)** Genome coverage of three biological replicates for Δ*rnhP rnhC::erm* strains. **(D)** Schematic of the *ppsA-E* operon. The location of the *pps* operon relative to the origin of replication, the operon length, and the orientation of transcription relative to replication are indicated. **(E)** Average genome coverage of WT (pink) and Δ*rnhP rnhC::erm,* Δ*ppsA-E* (light blue). The *ppsA-E* locus (1,960,230 – 1,997,989) is indicated by a black arrow.

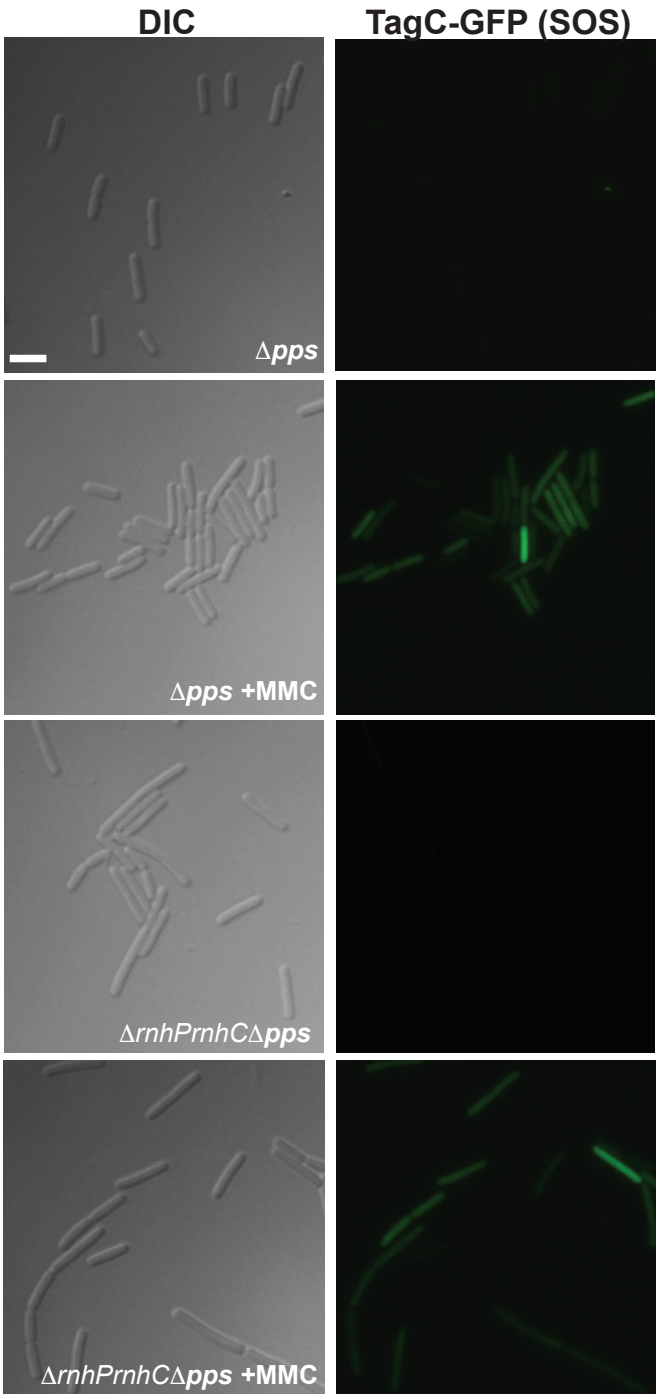

Figure S5. Cells with the Δ*pps* operon show reduced induction of the SOS response during normal growth. Shown are representative micrographs of *the tagC-gfp* reporter in cells with the Δ*ppsA-E* operon (TMN 141) or Δ*rnhP rnhC*::erm Δ*pps* strain (TMN 142) during normal growth and following treatment with mitomycin C. The percent of cells with SOS induction are summarized in a graph shown in Figure 6C of the main text. The white bar represents 3.4 μm.

Supplementary Table S1. Strains used in this study

Strains	Genotype	Source
TMN73	PY79 (wild type, SPβ°)	(Youngman *et al.*, 1984)
DK1042	NCIB 3610 comIQ12I	(Konkol *et al.*, 2013)
JWS207	PY79 Δ*rnhC*	(Yao *et al.*, 2013)
BKE28620	*rnhC::lox-erm-lox*	BGSC
BKE16060	*rnhB::lox-erm-lox*	BGSC
TMN107	DK1042 Δ*rnhC*	This work
DK7047	DK1042 Δ*rnhP*	This work
TMN110	DK1042 Δ*rnhP, rnhC::erm*	This work
TMN103	PY79 Δ*rnhC, amyE::Pspac-rnhP*	This work
TMN139	DK1042 *ΔppsA-E*	This work
TMN140	DK1042 *ΔppsA-E,* Δ*rnhP, rnhC::erm*	This work
TMN104	BL21 x pE-SUMO$_{zpdC(rnhP)}$	This work
TMN112	BL21 x pE-SUMO$_{zpdC(rnhP)D73N}$	This work
KJW7	PY79 *tagC::tagC-gfp*	(Britton *et al.*, 2007)
TMN115	DK1042 *tagC::tagC-gfp*	This work
TMN128	DK1042 Δ*rnhP,rnhC::erm, tagC::tagC-gfp*	This work
TMN141	DK1042 *tagC::tagC-gfp, ΔppsA-E*	This work
TMN142	DK1042 Δ*rnhP,rnhC::erm, tagC::tagC-gfp, ΔppsA-E*	This work
DK1634	Δ*PBSX* Δ*SPβ* Δ*comI amyE::hy$_{spank}$-zpdN*	(Myagmarjav *et al.*, 2016)
DK7765	Δ*PBSX* Δ*SPβ* Δ*comI* Δ*rnhP amyE::hy$_{spank}$-sigN*	This work
DK7814	Δ*PBSX* Δ*SPβ* Δ*comI* Δ*rnhP rnhC::erm amyE::hy$_{spank}$-sigN*	This work
DK786	comIQ12L *rnhC*::erm *amyE::hy$_{spank}$-sigN*	This work

Supplemental Table S2. Plasmids used in this study

Plasmid	Vector	Insert	Source
pTN_{rnhP1}	pDR110	*rnhP*	This study
pTN_{rnhP2}	pE-SUMO	*rnhP*	This study
pTN_{rnhP3}	pE-SUMO	*rnhP* D73N	This study
pAMB32	pMiniMAD2		(Patrick & Kearns, 2008)
pTNDpps	pPB105		This study

Supplemental Table S3. Oligos used in this study

Primer name	Primer sequence
oTN58	CGCGAACAGATTGGAGGTATGAAAAAGGTTGTAATT
oTN59	GTGGTGGTGCTCGATCATACGGCAGC
oTN60	CCCTGTAGAAATCAATACTAATTCTGCATATCTGTGCAAC
oTN61	GTTGCACAGATATGCAGAATTAGTATTGATTTCTACAGGG
oTN75	AAACAAAGAATAGCTGACTACTCTATAAGCCGCCG
oTN76	AAAACGGCGGCTTATAGAGTAGTCAGCTATTCTTT
oTN77	GCATGCTGAATTCGTAATGAGGTTCAAAAAACAAGGTATTACTGTGAAAGGGGAC
oTN78	TGGCCTCTGTCCGCTAATCCGCTCGGATTCCCTCCAGTTCTCATAATAAG
oTN79	ATTATGAGAACTGGAGGGAATCCGAGCGGATTAGCGGACAGAGG
oTN80	GCATAACCAAGCCTATGCCTACAGCTCTTCAATCATAAATGCAAGAGGATCATAGC
oJR209	/5IRD800CWN/CGATCGTAArGCTAGCTCTGC
oJR210	/5IRD800CWN/CGATCGTArArGrCrUAGCTCTGC
oJR227	/5IRD800CWN/rCrGrArUrCrGrUrArArGrCrUrArGrCrUrCrUrGrC
oJR145	GCAGAGCTAGCTTACGATCG
oJR339	rArGrUrArGrUrGrArArCrCrATGCTTACG/3IR800CWN/
oJR340	CGTAAGCATGGTTCACTACTCGCGCTTGATGC
oJR166	rGrCrArGrArGrArCrUrArGrCrUrUrArCrGrArUrCrG
oJR348	AGTAGTGAACCATGCTTACG/3IRD800CWN/
oJR365	CGTAAGCATGGTTCACTACT
oAB6715	AGGAGGAAGCTTGCCCGAAAATGATGATTATGG
oAB6716	CCTCCTGTCGACGTAAATTACAACCTTTTTCATTAAAG
oAB6717	AGGAGGGTCGACGCCGTATGAATGAATCAGTCTTC

oAB6718	CCTCCTGGTACCGAGCAATAGGATATGCCCGAC

Black and red text represents DNA and RNA sequences, respectively. IRDXXX represents infrared dye with excitation at 700 or 800 nM either at the 5' (5) or 3' (3) end of the oligo. CWN is NHS ester conjugation.

Supplemental Table S4. Additional growth curve parameters from Gompertz growth model.

	A	A CI	λ	λ CI
WT	2.51	(1.90-3.11)	111	(93-130)
Δ*rnhC*	1.88	(1.40-2.37)	104	(86-121)
Δ*rnhP*	2.09	(1.59-2.58)	105	(86-124)
Δ*rnhPrnhC::erm*	2.02	(1.57-2.46)	110	(94-126)

References

Britton, R.A., and Grossman, A.D. (1999) Synthetic lethal phenotypes caused by mutations affecting chromosome partitioning in Bacillus subtilis. *J Bacteriol* **181**: 5860-5864.

Britton, R.A., Kuster-Schock, E., Auchtung, T.A., and Grossman, A.D. (2007) SOS induction in a subpopulation of structural maintenance of chromosome (Smc) mutant cells in Bacillus subtilis. *J Bacteriol* **189**: 4359-4366.

Burby, P.E., and Simmons, L.A. (2016) MutS2 promotes homologous recombination in Bacillus subtilis. *J Bacteriol*. 199(2):e00682-16.

Burby, P.E., and Simmons, L.A. (2017) CRISPR/Cas9 Editing of the Bacillus subtilis Genome. *Bio Protoc* **7**.

Konkol, M.A., Blair, K.M., and Kearns, D.B. (2013) Plasmid-encoded ComI inhibits competence in the ancestral 3610 strain of Bacillus subtilis. *J Bacteriol* **195**: 4085-4093.

Koo, B.M., Kritikos, G., Farelli, J.D., Todor, H., Tong, K., Kimsey, H., Wapinski, I., Galardini, M., Cabal, A., Peters, J.M., Hachmann, A.B., Rudner, D.Z., Allen, K.N., Typas, A., and Gross, C.A. (2017) Construction and Analysis of Two Genome-Scale Deletion Libraries for Bacillus subtilis. *Cell Syst* **4**: 291-305 e297.

Li, H., and Durbin, R. (2009) Fast and accurate short read alignment with Burrows-Wheeler transform. *Bioinformatics* **25**: 1754-1760.

Li, H., Handsaker, B., Wysoker, A., Fennell, T., Ruan, J., Homer, N., Marth, G., Abecasis, G., Durbin, R., and Genome Project Data Processing, S. (2009) The Sequence Alignment/Map format and SAMtools. *Bioinformatics* **25**: 2078-2079.

Myagmarjav, B.E., Konkol, M.A., Ramsey, J., Mukhopadhyay, S., and Kearns, D.B. (2016) ZpdN, a Plasmid-Encoded Sigma Factor Homolog, Induces pBS32-Dependent Cell Death in Bacillus subtilis. *J Bacteriol* **198**: 2975-2984.

Nye, T.M., Schroeder, J.W., Kearns, D.B., and Simmons, L.A. (2017) Complete Genome Sequence of Undomesticated Bacillus subtilis Strain NCIB 3610. *Genome Announc* **5**: pii: e00364-00317.

Patrick, J.E., and Kearns, D.B. (2008) MinJ (YvjD) is a topological determinant of cell division in Bacillus subtilis. *Mol Microbiol* **70**: 1166-1179.

Quinlan, A.R., and Hall, I.M. (2010) BEDTools: a flexible suite of utilities for comparing genomic features. *Bioinformatics* **26**: 841-842.

Wickham, H., (2016) *ggplot2: Elegant Graphics for Data Analysis*. Springer-Verlag, New York.

Yao, N.Y., Schroeder, J.W., Yurieva, O., Simmons, L.A., and O'Donnell, M.E. (2013) Cost of rNTP/dNTP pool imbalance at the replication fork. *Proceedings of the National Academy of Sciences of the United States of America* **110**: 12942-12947.

Yasbin, R.E., and Young, F.E. (1974) Transduction in Bacillus subtilis by bacteriophage SPP1. *J Virol* **14**: 1343-1348.

Youngman, P., Perkins, J.B., and Losick, R. (1984) Construction of a cloning site near one end of Tn917 into which foreign DNA may be inserted without affecting transposition in Bacillus subtilis or expression of the transposon-borne erm gene. *Plasmid* **12**: 1-9.

Zeileis, A., and Grothendieck, G. (2005) zoo: S3 Infrastructure for Regular and Irregular Time Series. *Journal of Statistical Software* **14**:1-27